Chapter 1

The ATLAS Experiment at the Large Hadron Collider LHC

1.1 ATLAS Physics Analysis

Since long the MPP ATLAS group continuously works on the preparation of physics analysis of hadron collision data at the LHC. The results obtained in the years 1997-2007, including preparatory work based on Tevatron data, are described in the previous reports [1, 2, 3], and references therein.

The present physics studies for the ATLAS experiment cover a broad physics range. Already at this early stage of data taking, a number of Standard Model (SM) processes occur in abundance. These processes allow for detailed studies of the detector performance, as well as for the precision measurement of QCD and electroweak observables. In this respect the top-quark physics is of particular interest. A good understanding of SM processes is essential also for new discoveries. The ATLAS discovery potential is explored in searches for the Higgs boson both in the Standard Model and in supersymmetric extensions, as well as in a generic search for supersymmetric particles. The ongoing investigations are described in more detail below.

1.1.1 Measurement of Standard Model Processes

Measurement of Inclusive Lepton Cross Sections

At the LHC pp collision events with highly energy electrons and muons in the final provide clean signatures for many physics processes of interest. A good understanding of the inclusive electron and muon cross section is therefore of great importance. The MPI group contributes to the measurement of the inclusive electron and muon cross section [4, 5, 6].

At the LHC electrons are produced predominantly produced in decays of heavy quarks for transverse momenta below about 30 GeV/c and in decays of W and Z boson at higher transverse momenta. The MPI group significantly contributed to the optimization of the electron selection criteria to arrive at an electron selection efficiency which is flat in the transverse electron momentum (see Figure 1.1). The first measured inclusive electrons spectrum at a centre-of-mass energy of 7 TeV at the LHC shown in Figure 1.2 agrees with the prediction of the Pythia minimum bias Monte-Carlo prediction within about 20%. The MPI group contributes to the analysis of this discrepancy with increasing statistics of the inclusive electron sample.

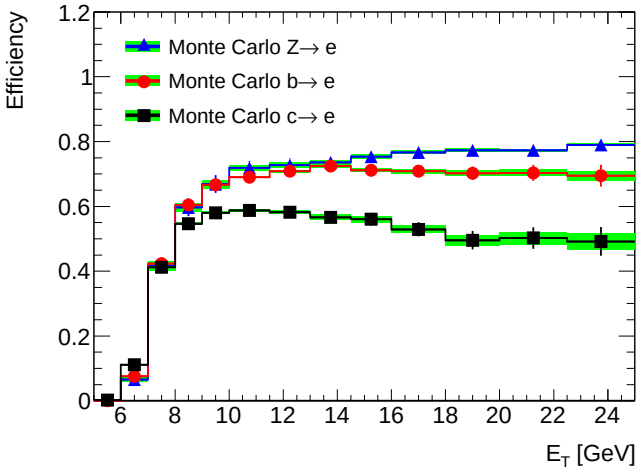

Figure 1.1: Monte-Carlo prediction of electron reconstruction efficiency for electrons from heavy quark and Z boson decays after the optimization of the electron identification cuts.

The MPI group is also involved in the measurement of the inclusive muon cross section contributing with its experience in muon performance studies. The measured inclusive muon p_T spectrum is presented in Figure 1.3 where it is compared with the Pythia

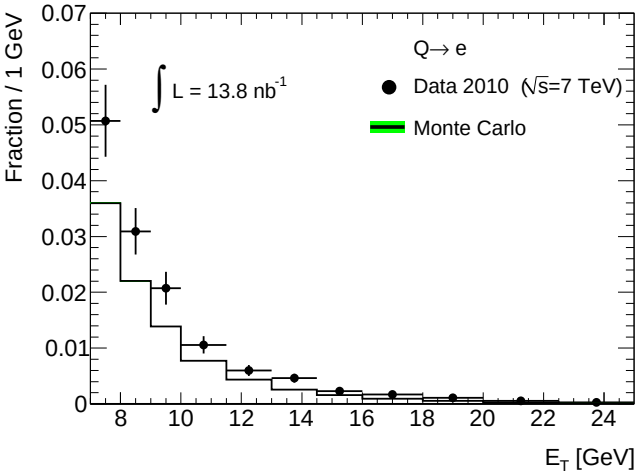

Figure 1.2: Comparison of the measured distribution of the transverse energies of prompt electrons from c and b decays with the Pythia 6.4 minimum bias Monte-Carlo predictions.

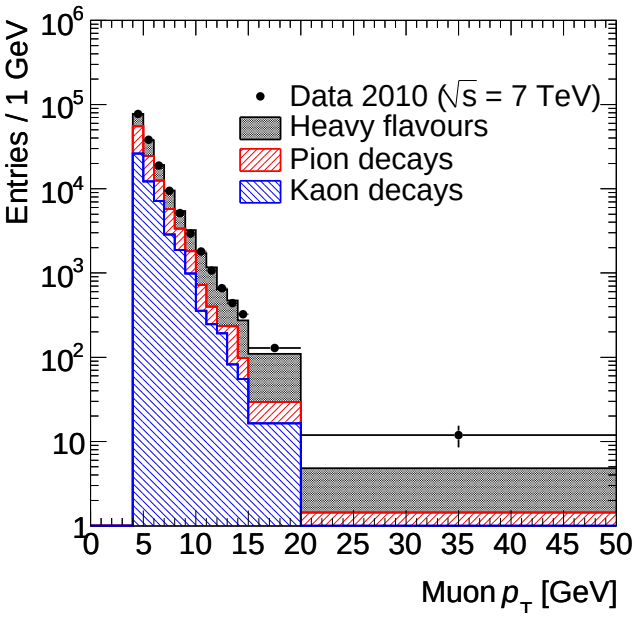

Figure 1.3: Comparison of the measured inclusive muon transverse momentum spectrum with the Pythia 6.4 minimum bias Monte-Carlo prediction. The Monte-Carlo data is decomposed into the three sources of muons, namely in-flight decays of charged pions and kaons and the decays of heavy-flavour hadrons.

6.4 minimum bias Monte-Carlo prediction. The measured spectrum is well reproduced by the Monte-Carlo simulation. The main sources of the muon at transverse momenta below 20 GeV/c are in-flight decays of charged pions and kaons and the decays of heavy-flavour hadrons according to the Monte-Carlo simulation. Decays of W and Z bosons become important for $p_T > 20$ GeV/c. The contribution of pion and kaon decays in-flight to the inclusive muon spectrometer will be estimated from data by comparing the momentum measured in the inner detector with the momentum measured in the muon spectrometer. For late pion and kaon decays in the inner detector lead to a large momentum inbalance between the inner detector and muon spectrometer as illustrated in Figure 1.4.

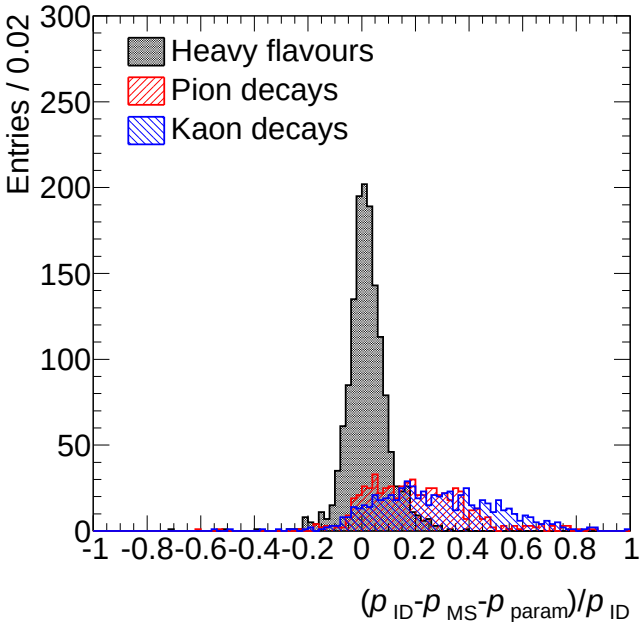

Figure 1.4: Distribution of the difference of the muon momentum measurements in the inner detector and the muon spectrometer normalized to the inner detector momentum measurements in simulated data. Decays of pions and kaons in flight lead to a large tail to positive values as the inner detector measures the pion and kaon momentum while the muon spectrometer measures the momentum of the decay muon.

Study of Processes with Electroweak Gauge Bosons

Standard Model processes are studied with the motivation of estimating the backgrounds to the production of Higgs bosons and supersymmetric particles from the data and to improve the Monte Carlo simulations. The processes under investigation are QCD high p_T and multi-jet production, forward jet production, b jet production, inclusive W, Z and $t\bar{t}$ production as well as $Z \rightarrow \tau^+\tau^-$ decays. $Z \rightarrow e^+e^-$ and $\mu^+\mu^-$ decays are being studied for the purpose of detector calibration and data quality monitoring. The analysis methods developed will be applied to first measurements of multi-jet, $b\bar{b}$ and inclusive W and Z production cross-sections with the early data.

Figure 1.5 shows the transverse mass distribution of the $W \rightarrow \mu\nu_\mu$ candidates in the first 16.6q nb^{-1} of pp

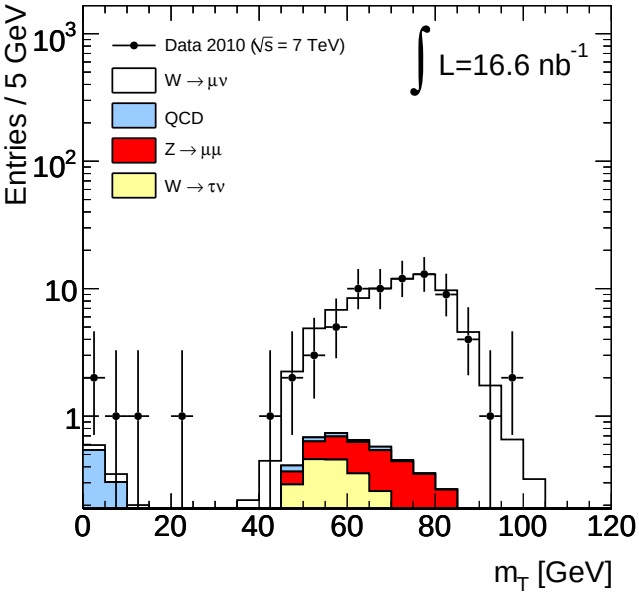

Figure 1.5: Transverse mass distribution of $W \rightarrow \mu\nu_\mu$ candidates found in the first 16 nb^{-1} of pp collision data collected by ATLAS.

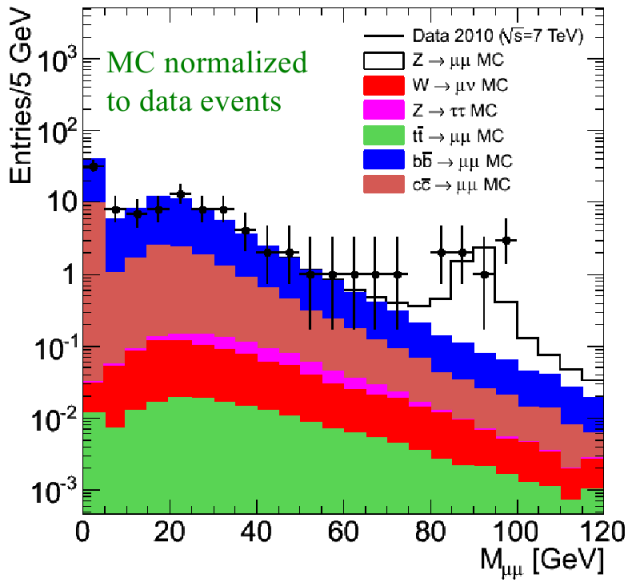

Figure 1.6: Invariant dimuon invariant mass distribution for isolated muonss in the first 16 nb^{-1} of pp collision data collected by ATLAS. An excess of 8 Z events is visible in the distribution consistent with the Monte-Carlo prediction.

collision data collected by ATLAS. The measured distribution is consistent with the Monte-Carlo prediction and has a negligible background contamination. In the same set of pp collision data ATLAS has observed 8 Z boson candidates as can be seen as an excess of entries at the Z mass in the dimuon mass spectrum of Figure 1.6 [7].

A first measurement of the W production cross section could also performed and is summarized in Table 1.7.

1.1.2 Top-Quark Physics

Overview

The top-quark is by far the heaviest known elementary building block of matter. The precise knowledge of the quantum numbers of the top-quark helps to further constrain the parameters of the Standard Model, and is a mandatory prerequisite for any study of new physics that will almost inevitably suffer from top-quark reactions as background processes. In addition, the top-quark should have the strongest couplings to any mechanism that generates mass, which makes it a very interesting object for an unbiased search for this mechanism.

The present main interest of the top-quark physics analysis work of the MPP group is the investigation of the $t\bar{t}$ production process, and particularly the determination of the mass of the top-quark (m_{top}) and the production cross-section ($\sigma_{t\bar{t}}$) in the reaction $t\,\bar{t} \rightarrow b\,\bar{b}\,W^+\,W^-$.

The analyses use two decay channels of the W-boson pair, the lepton + jets channel, where the W-boson pair decays into $\ell\nu\,qq'$ with $\ell = e,\ \mu$ (branching ratio, $\mathcal{BR} = 30\%$) and the all-jets channel, where both W-bosons decay into a qq' pair ($\mathcal{BR} = 44\%$). In both channels m_{top} is obtained from hadronically decaying W-bosons and the corresponding b-jet.

The main background reactions to $t\,\bar{t}$ production, as determined from Monte Carlo simulations, are the W + n-jets production, QCD multijet production, single top-quark production, and that fraction of the $t\bar{t}$ production where the W-boson pair decays via the other decay channels. The QCD multijet production process is special due to the huge cross-section before any cut, such that event samples fully covering the signal phase space cannot be simulated with sufficient statistics, especially for the lepton + jets channel, where the selected lepton mostly results from a wrongly reconstructed jet. Eventually this background contribution has to be obtained from data. So far, initial studies of this background based on Monte Carlo samples have been performed and methods to evaluate it from the data, like the matrix-method, have been implemented. The matrix-method was successfully applied to estimate the background fraction from Monte Carlo samples with a deliberately unknown composi-

	W^+				W^-				$W^\pm$			
Electron channel												
	value	stat	syst	lumi	value	stat	syst	lumi	value	stat	syst	lumi
Background-subtracted signal	25.6	4.8	0.3	0.1	17.8	3.8	0.3	0.1	43.4	5.9	0.4	0.2
Correction C_W	0.653	-	0.033	-	0.660	-	0.033	-	0.656	-	0.033	-
Fiducial cross section (nb)	**2.3**	0.4	0.1	0.3	**1.6**	0.3	0.1	0.2	**3.9**	0.5	0.1	0.4
Acceptance A_W	0.466	-	0.014	-	0.457	-	0.014	-	0.462	-	0.014	-
Total cross section (nb)	**5.1**	0.9	0.3	0.6	**3.4**	0.7	0.2	0.4	**8.4**	1.2	0.4	0.9
Muon channel												
	value	stat	syst	lumi	value	stat	syst	lumi	value	stat	syst	lumi
Background-subtracted signal	43.8	6.9	0.6	0.3	22.8	5.0	0.3	0.2	66.7	8.5	0.7	0.5
Correction C_W	0.822	-	0.057	-	0.804	-	0.057	-	0.814	-	0.056	-
Fiducial cross section (nb)	**3.2**	0.5	0.2	0.4	**1.7**	0.4	0.1	0.2	**4.9**	0.6	0.4	0.5
Acceptance A_W	0.484	-	0.014	-	0.475	-	0.014	-	0.480	-	0.014	-
Total cross section (nb)	**6.6**	1.0	0.5	0.7	**3.6**	0.8	0.3	0.4	**10.3**	1.3	0.8	1.1

Figure 1.7: Results for the fiducial cross sections σ_{fig} (for $|\eta| < 2.5$) and total cross section σ_{tot} for W^+, W^-, and $W^\pm$ in the electron and muon channels. Shown are the observed numbers of signal events after background subtraction for each channel, the average corrections factor C_W, the fiducial cross sections, the geometrical acceptance correction factors, and the total cross sections with their statistical, systematic, and luminosisty uncertainties quoted in that order.

tion of signal and background events [8]. In the MPP investigations, for the first time the k_t-jet algorithm has been used in top physics analyses at ATLAS [**?**, 9] Because of a better stability against divergences, this algorithm is theoretically preferred over the traditionally applied cone-jet algorithm. By now also the experimental advantages became apparent, such that since recently a variant of it, namely the anti-k_t jet algorithm is the ATLAS standard.

At present the analyses are optimized on Monte Carlo samples and are ready to be applied to the data to be taken still this year. The analyses are mostly performed assuming the initially envisaged proton-proton center of mass energy of $\sqrt{s} = 10\,\text{TeV}$ and for integrated luminosities $\mathcal{L}_{\text{int}}$ of several 100 pb^{-1}. An overview of the recent activities is given below, the initial investigations were reported in [2, 3].

Lepton + Jets Channel

The lepton + jets channel is the best compromise of branching fraction and signal-to-background ratio (S/B), defined as the ratio of $t\bar{t}$ signal events to physics background events. Therefore most of the effort is invested in this channel. At MPP a number of analyses have been performed to arrive at the most sensitive observable and analysis strategy for obtaining m_{top} from the invariant mass of the three jets assigned to the decay products of the hadronically decaying top-quark. Different event- and jet selection algorithms, observables, jet calibration schemes (see Sec. **??**), and fitting methods have been exploited for this.

In the lepton + jets channel the charged lepton with a high transverse momentum[1] (p_{T}) from the decay

[1] In the ATLAS right-handed coordinate system the x-axis points towards the center of the LHC ring, the y-axis points upwards and the z-axis points in the direction of the counter-clockwise running proton beam. The polar angle θ and the azimuthal angle ϕ are defined with respect to the z-axis and

of one W-boson is utilized to trigger and identify the event, and to efficiently suppress background without genuine charged leptons, i.e. from the QCD multijet production. In general, the event selection for the lepton + jets channel requires an isolated electron or muon within the good acceptance of the detectors, which has a transverse momentum of more that 20 GeV and lies within the rapidity range of $|\eta| < 2.5$. Since the initial state is balanced in p_T, to account for the neutrino a missing transverse energy of more than 20 GeV is required. In addition, at least four jets are required within the same range of rapidity, and having transverse momenta of more than 40 GeV for the three highest p_T jets, and more than 20 GeV for the fourth jet. All jets should be well separated from the identified lepton. Given the different emphasis of the analyses, these requirements are slightly modified or additional requirements like the presence of identified b-jets, or restrictions to the reconstructed invariant mass of the W-boson are imposed. With these selections, for each lepton sample an average signal efficiency of about 10% is reached, and the S/B is about 1.5.

The standard assignment of jets to the top-quark and the W-Boson are as follows. For each event, from all jets with $p_T > 20$ GeV the three jet combination which maximizes the transverse momentum is chosen to form the hadronically decaying top-quark. This algorithm is named the p_T-max method. Out of this, the two jet pair with the smallest ΔR is taken to represent the W-boson. A typical top-quark mass spectrum observed with these requirements [**?**], and only using signal events and W + n-jets events, is shown in Fig. 1.8. In this example, the spectrum is fitted with a Gaussian function to parameterize the correct combinations leading to the top-quark mass and width, and a sum of Chebyshev polynomials used to describe the events stemming from the sum of the physics background events and wrong jet combinations in selected signal events. The Gaussian part of the fit is also shown separately and compared to the red histogram made from the correct jet triplet. In this case correct jet triplets are defined as those combinations of jets where the reconstructed four-vector of the jet triplet coincides with that of the top-quark to within $\Delta R = 0.1$.

From this figure it is clear that firstly the correct jet triplets constitute only a small part of the events in the peak region around the generated top-quark mass

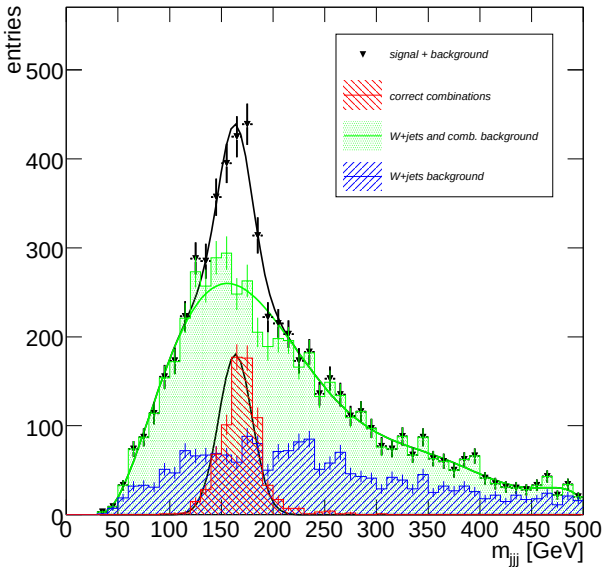

Figure 1.8: The reconstructed top-quark mass together with a fit.

of 172.5 GeV, secondly that the shape of the combinatorial background can well influence the fitted peak value, and thirdly that the shown W + n-jets contribution is still sizeable and not entirely flat.

These issues are addressed, e.g. by using other algorithms to select the jet triplet, or by exploiting additional variables or a constrained fit that both help to separate signal from background. Additional algorithms studied include the so-called ΔR method that exploits the angular correlations between the two b-jets that should have a large ΔR, and the two light-jets that should have a small ΔR. This algorithm works without explicitly using b-jet identification, instead from a p_T ordered jet list the first two jets are assumed to be the b-jets and the next two jets to stem from the W-Boson decay. On these jets the angular requirements are applied. Whether the decrease in statistical precision compared to the p_T-max method is compensated by superior features like an improved resolution, or a smaller bias in the reconstructed mass, is under investigation.

Due to the presence of the decay of the top-quarks that correlate the W-Bosons and their corresponding b-quarks, the signal events should exhibit a different correlation of the observed jet structure than the background processes without top-quarks. The separation of the jets can be monitored when running the k_t-jet algorithm by studying the $d_{\text{merge}}(M \rightarrow M-1)$ values at which an M-jet configuration is reduced to an $(M-1)$-jet configuration. In a multivariate analysis

x-axis, respectively. The pseudo-rapidity is defined as $\eta = -\ln(\tan(\theta/2))$ and the radial distance in (η, ϕ) space is $\Delta R = \sqrt{\Delta\eta^2 + \Delta\phi^2}$.

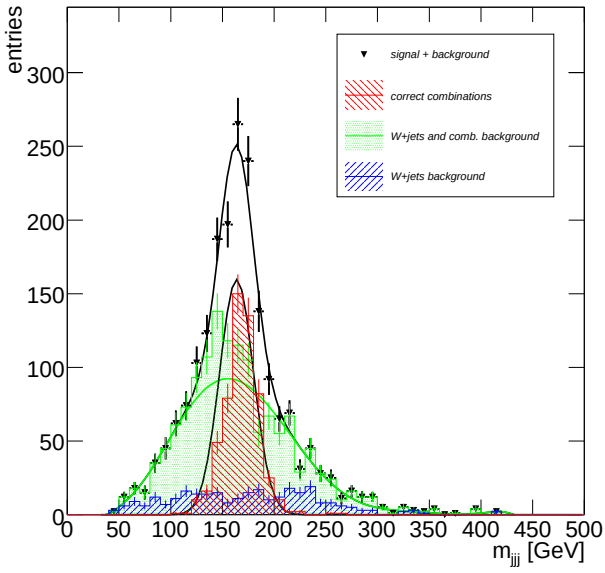

Figure 1.9: Same as Fig. 1.8 but with an additional likelihood selection.

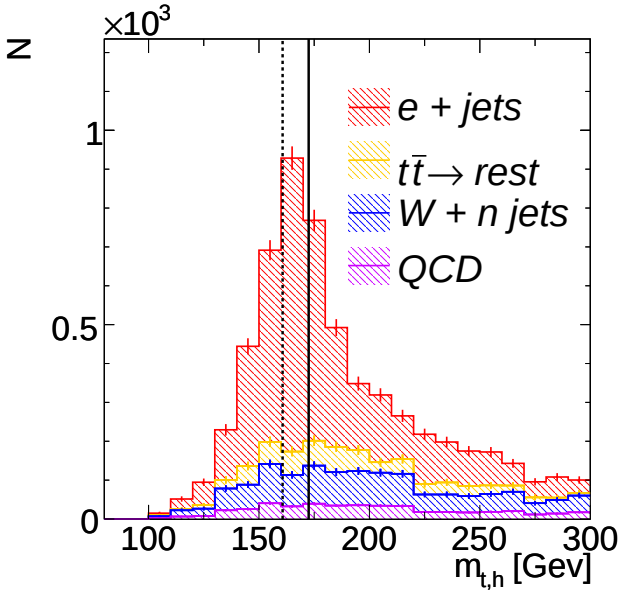

Figure 1.10: The top-quark mass distribution when applying a constrained fit selection.

it was found that the d_{merge} values in signal and background events are not sufficiently different to be used as discriminating variables [**?**]. In contrast, a likelihood function build from seven event variables, like e.g. the invariant mass of the charged lepton and its assigned b-jet, or the ΔR between the W-Boson and the b-jet from the hadronically decaying top-quark candidate, is clearly able to significantly improve the S/B, while retaining most of the events where the correct jet triplet was selected. This is demonstrated in Fig. 1.9.

A kinematic fit exploiting as constraints the known W-Boson mass both for the leptonic and the hadronic W-Boson decays, and in addition the equality of the two corresponding reconstructed top-quark masses mainly serves three purposes. Firstly, it increases the efficiency for selecting the correct jet triplet by making more detailed use of the entire event. Secondly, it provides a quality measure, namely the probability $P(\chi^2)$ of the fit, to better suppress background events. Finally, it improves on the resolution of the top-quark mass provided the uncertainties of the measured quantities and their correlations are properly understood, something that is only expected after a larger data set has been analyzed. Compared to the p_{T}-max method the efficiency for selecting the correct jet triplet is increased by about 15% absolute, and about 25% of the background events can be removed [10] by requiring $P(\chi^2) > 0.15$. An example of such a selection for events with four reconstructed jets and requiring $P(\chi^2) > 0.15$ is shown in Fig. 1.10. The better suppression of the W + n-jets events compared to Fig. 1.8 is apparent. It has been verified that this improvement, is very stable against variations of the assumed object resolutions. Since at the moment only initial approximations are made for the resolution of the objects, the possible improvement in the mass resolution is not yet exploited.

The largest systematic uncertainty in any determination of m_{top} stems from the imperfect knowledge of the jet energy scale (JES), which depends on kinematic properties like p_{T} and η of the jets, and is different for light-jets and b-jets. Therefore, one of the most important features of any m_{top} estimator is the stability against the variation of the JES. To minimize the JES uncertainty on the measured m_{top} two paths are followed: one is a calibration by means of the known W-boson mass ($M_{\text{W}}^{\text{PDG}}$) to obtain the JES for light-jets, the other is exploring the stabilized top-quark mass ($m_{\text{top}}^{\text{stab}}$, see below) to be as independent as possible of the actual JES value, without actually determining it.

In the lepton + jets channel an iterative in-situ calibration of the JES for the selected events has been performed [11]. Jets are treated in the massless limit with unchanged reconstructed angles, such that any change in the invariant two-jet mass ($M_{\text{W}}^{\text{reco}}$) can be expressed in energy dependent JES factors. The jet calibration then makes use of the fact that $M_{\text{W}}^{\text{reco}}$ calculated from the jets assigned to the W-boson decay has to match $M_{\text{W}}^{\text{PDG}}$. The energy bins are chosen logarithmically from 50 GeV to 400 GeV and the resulting calibration

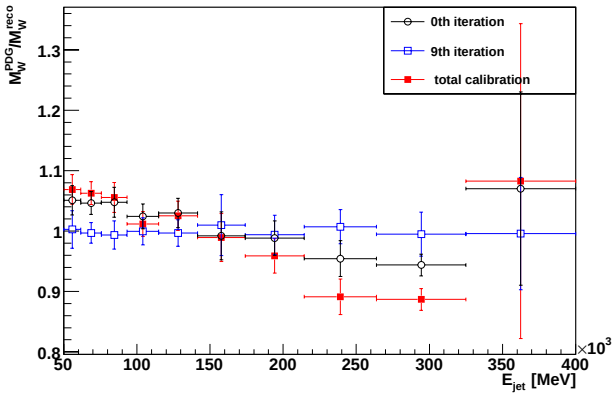

Figure 1.11: In-situ calibration of the W-Boson mass as function of the light-jet energy.

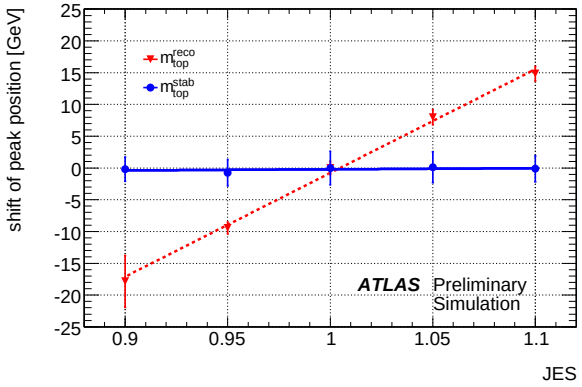

Figure 1.12: Stability of $m_{\text{top}}^{\text{reco}}$ and $m_{\text{top}}^{\text{stab}}$ against JES changes.

factors, which are consecutively applied per iteration, are shown in Fig. 1.11 for the initial situation, the 9$^{\text{th}}$ iteration and the final result. The flatness of the calibration factors of the 9$^{\text{th}}$ iteration with values close to unity clearly shows that the fit has converged. Comparing the initial and final situation reveals that the iterations slightly change the simple picture one would have obtained by once adjusting the peak of the initial distribution to $M_{\text{W}}^{\text{PDG}}$. When applying this global scaling method the uncertainty on m_{top} from the JES uncertainty is considerably reduced [11].

The variable $m_{\text{top}}^{\text{stab}}$ is calculated as the ratio of the reconstructed masses of the top-quark and the W-Boson candidates from the selected jet triplet. For convenience this ratio is multiplied by $M_{\text{W}}^{\text{PDG}}$. The main consequence of using $m_{\text{top}}^{\text{stab}}$ is a strong event-by-event cancellation of the JES dependence of the three-jet and two-jet masses in the mass ratio, while retaining the sensitivity to m_{top}. The quantitative gain in stability when using $m_{\text{top}}^{\text{stab}}$ instead of the jet triplet invariant mass $m_{\text{top}}^{\text{reco}}$ is apparent from Fig. 1.12 taken from [12] Using this variable a template analysis has been developed [8, 13, 12]. In this analysis Probability Density Functions (PDFs) are constructed from templates of the signal events at various assumed m_{top} values and from a template of the combined physics background events. The signal PDF linearly depends on m_{top}, whereas the background PDF does not. Using pseudo-experiments for a given luminosity the sensitivity of the method, together with the systematic uncertainties from various sources, has been estimated. An example of a pseudo experiment is shown in Fig. 1.13 for the muon channel and for $\sqrt{s} = 10\,\text{TeV}$ and $\mathcal{L}_{\text{int}} = 100\,\text{pb}^{-1}$. For this situation the statistical uncertainty for the combined electron and muon channel is about

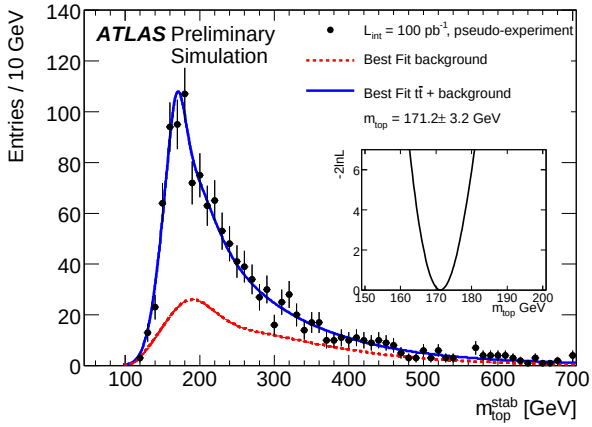

Figure 1.13: Pseudo-experiment mimicking early ATLAS data in the muon channel.

2 GeV. The total systematic uncertainty is estimated to be about 3.8 GeV for each channel, still dominated by the systematic uncertainty from the JES for light jets and b-jets [12].

The determination of the combinatorial- and physics background from data rather than from Monte Carlo samples likely results in a reduced systematic uncertainty. For this purpose a data driven method was developed that explores the $m_{\text{top}}^{\text{reco}}$ and $R_{\text{top}} = m_{\text{top}}^{\text{reco}}/M_{\text{W}}^{\text{reco}}$ distributions at the same time. The idea is to use e.g. the events from the sideband region of the $m_{\text{top}}^{\text{reco}}$ distribution to predict the shape of the background contribution to the R_{top} distribution. An initial investigation ignoring possible shape differences of the combinatorial- and physics background, and using a simple four-vector smearing approach, yields promising results, and will be extended to fully simulated Monte Carlo events and eventually data.

A direct fit to the $m_{\text{top}}^{\text{reco}}$ distribution and the tem-

plate method lead to different systematic uncertainties. An analysis is underway to systematically compare the two approaches. This is done for the p_T-max and for a selection method that defines the top-quark as the jet triplet with the minimum sum of the three ΔR values.

Concerning the cross-section measurement an initial investigation of a cut and count analyses with and without using b-jet identification has been performed [14]. It exploits the lepton + jets channel at $\sqrt{s} = 10\,\text{TeV}$ and for $\mathcal{L}_{\text{int}} = 200\,\text{pb}^{-1}$. Within the systematic uncertainties investigated the total systematic uncertainty estimated is about 30%.

All-Jets Channel

In the all-jets channel only jet requirements and jet topologies can be used to separate the signal from the background reactions. Consequently, this channel suffers from a much higher background from the QCD multijet production. Here, events with isolated leptons are vetoed, and the missing transverse energy is required to be consistent with zero. In addition, at least six jets, not consistent with being purely electromagnetic, and two of which are identified b-jets, are required within $|\eta| < 2.5$. By exploring the transverse energies of the jets and the angular correlation of the two b-jets, the S/B is improved by several orders of magnitude to about 10^{-1}, while retaining a signal efficiency of about 10%. In this procedure the use of b-jet identification is absolutely essential. In addition, the availability of a multi-jet trigger with appropriate thresholds is imperative to not loose the signal events already at the trigger stage. This involves a delicate optimization to retain a sufficiently high efficiency for the signal events, while not saturating the ATLAS readout system with the QCD multijet events. The trigger conditions have been carefully studied, and the use of some trigger signals are suggested to ATLAS. Under the assumption that these will be available, and when exploiting the above event selection, a mass distribution has been isolated, where the signal starts to be visible on a still large background. For this analysis the next steps are the optimization of the background description and a fit to the distribution to access the sensitivity to m_{top}.

Summary

In summary the MPP analyses in the Top Physics area are well advanced. A variety of paths are explored in the search for the most appropriate variable and analysis strategy to determine the top-quark mass, a measurement that will soon be dominated by the systematic uncertainty. The methods in hand allow for a cross-calibration of the result for gaining confidence in their stability. Members of the group are actively participating in the ATLAS efforts, and have presented Top Physics results from the MPP group and beyond at international conferences [15, 16]

1.1.3 Searches for the Higgs Boson

The origin of particle masses is one of the most important open questions in particle physics. In the Standard Model (SM), the answer to this question is connected with the prediction of a new elementary particle with neutral charge, the Higgs boson H. The mass m_H of the Higgs boson is an unknown parameter of the theory. The experimental lower bound of 115 GeV has been set by the LEP experiments, while the recent searches at the Tevatron have excluded a SM Higgs boson in the mass range of $162 < m_H < 166$ GeV. The theoretical upper limit of about 800 GeV still leaves a wide mass range to be explored.

In the minimal supersymmetric extension of the Standard Model (MSSM), the Higgs mechanism predicts the existence of five Higgs bosons, three neutral ($h/H/A$) and two charged ones $H^{\pm}$. Their production cross-sections and decays are determined by two independent parameters, e.g. the ratio $\tan\beta$ of the vacuum expectation values of the two Higgs doublets in this model and the mass m_A of the pseudoscalar Higgs boson. Current experimental searches at LEP and Tevatron exclude at a 95% confidence level the A boson mass values below 93 GeV, as well as the $\tan\beta$ values below 2. For an A boson mass of up to 200 GeV, also the high $\tan\beta$ values above 40 are excluded.

The search for the Higgs boson is one of the main motivations for the LHC and the ATLAS experiment. The high cross sections of the background processes exceeding the signal by many orders of magnitude call for selective triggers, efficient background suppression and reliable prediction of the background contributions. Until recently, our studies were devoted to the preparation for an early Higgs boson discovery during the first years of LHC running at the nominal center-of-mass collision energy of 14 TeV. The obtained results can be found in the newly published review of the ATLAS physics potential [17]. As of lately, the searches are being optimized for the initial LHC operation at a centerer-of-mass energy of 7 TeV. With a relatively low expected total integrated luminosity of

1 fb^{-1}, the Higgs boson discovery is rather unlikely under these operating conditions. However, the allowed Higgs mass range can be constrained beyond the present experimental limits, as summarized in [18].

The Standard Model Higgs Boson

The expected potential for the Standard Model Higgs boson discovery is shown in Fig. 1.14. In the mass range above 180 GeV, the key discovery channel is the Higgs decay into four charged leptons via two intermediate Z bosons. The lower mass range can only be covered by the combination of searches in several Higgs decay modes.

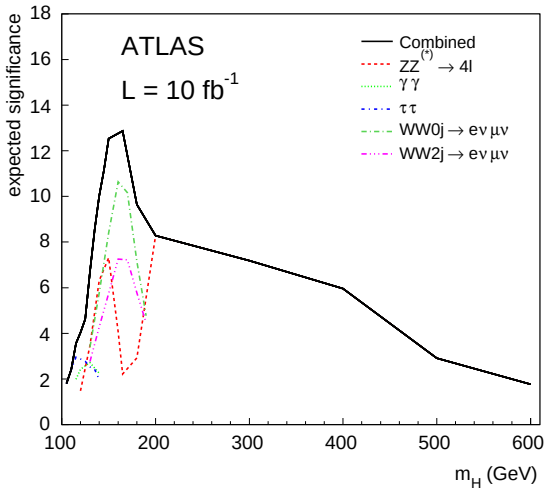

Figure 1.14: Discovery potential of the ATLAS experiment for the Standard Model Higgs boson. The statistical significance expected for an integrated luminosity of 10 fb^{-1} at a centerer of mass energy of 14 TeV is shown for the different Higgs decay modes and their combination as a function of the Higgs boson mass m_H.

The clearest signature is found in the four-lepton decay channel $H \to ZZ^{(*)} \to 4\ell$ which also allows for a precise Higgs mass measurement. The reconstruction of this channel strongly relies on the high lepton identification efficiency and good momentum resolution of the ATLAS detector. The reducible $Zb\bar{b}$ and $t\bar{t}$ background processes can be suppressed by means of the Z boson mass reconstruction and the requirement of a low jet activity in the vicinity of each lepton. The remaining reducible background is small compared to the irreducible $ZZ^{(*)}$ background. In addition to the optimization of the analysis selection criteria, our studies include the detailed evaluation of the theoretical and experimental systematic uncertainties for both signal and background processes [19]. We also evaluate the potential to exclude a part of the allowed Higgs mass range in the initial phase of LHC operation [20], including the development of the methods for the precise determination of the background contributions from data. The expected exclusion limits are shown in Fig. 1.15 (top picture). The best upper limit on the Higgs boson production, obtained for the Higgs mass around 200 GeV, is still about a factor of two above the Standard Model prediction. The exclusion reach is especially low in the mass region around 160 GeV, where the $H \to ZZ^*$ decays are strongly suppressed by the Higgs boson decays into two on-shell W bosons.

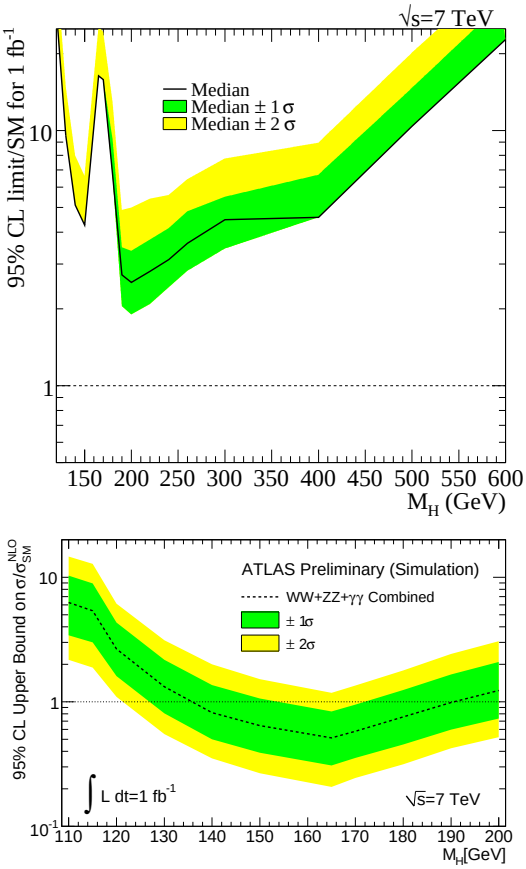

Figure 1.15: Expected upper limits (95% confidence level) on the Standard Model Higgs boson production rate in the $H \to ZZ^{(*)} \to 4\ell$ channel alone (top picture) and after the combination with the $H \to WW \to \ell\nu\ell\nu$ and $H \to \gamma\gamma$ channels (bottom picture), shown as a function of the Higgs mass at an integrated luminosity of 1 fb^{-1} and a centre-of-mass energy of 7 TeV and normalized to the Standard Model prediction. The bands indicate the 68% and 95% probability regions in which the limit is expected to fluctuate in the absence of signal.

Due to the high branching ratio for the decay $H \to$

$W^+W^- \rightarrow (\ell\nu)(\ell\nu)$, the Higgs boson with a mass between 140 GeV and 180 GeV can be excluded in this channel during the initial phase of LHC operation. In combination with the four-lepton decay channel, the exclusion reach is slightly improved to cover the mass range from 135 GeV to 190 GeV, as shown in Fig. 1.15 (bottom picture). Due to the two neutrinos in the final state of the Higgs decays into W bosons, no precise measurement of the Higgs mass is possible. Precise determination of the background contributions is therefore required to exclude the presence of signal events. For this purpose, we are measuring the Standard Model background processes with present LHC data. The $H \rightarrow WW$ decay channel also allows for an early Higgs boson discovery during the LHC operation at 14 TeV. Parallel to the optimization of the event selection criteria in this context [21], we have developed a new algorithm for the jet reconstruction [22, 23], which is used for the suppression of the $t\bar{t}$ and $W+jets$ backgrounds to the Higgs production via the W or Z gauge boson fusion. The algorithm reconstructs the jets using particle tracks in the inner detector instead of energy deposition in the calorimeters. The inner detector tracks can be associated to common vertices leading to a jet reconstruction probability which is insensitive to the presence of multiple proton-proton interactions per beam collision (pile-up events).

In the mass range below 140 GeV, the Higgs boson predominantly decays into $b\bar{b}$ pairs. Due to the large contribution of QCD background in the gluon-fusion production mode, this decay can only be triggered and discriminated from the background in the production mode of the Higgs boson in association with a $t\bar{t}$ pair. Our studies have shown that the discovery potential in the $H \rightarrow b\bar{b}$ decay channel is very much limited by the large experimental systematic uncertainties [24, 25].

The second most frequent mode which can be observed in the mass range below 140 GeV is the decay into a $\tau^+\tau^-$ pair. This decay can only be discriminated against the background processes in the Higgs production mode via the W or Z gauge boson fusion where two additional forward jets in the final state provide a signature for background rejection. The decay modes with both τ leptons decaying leptonically ($\ell\ell$ mode) as well as with one hadronic and one leptonic τ-decay (ℓh mode) have been studied ([26], [27]). The event selection criteria have been optimized using multivariate analysis techniques. With a neural network based background rejection method, the signal significance is improved compared to the standard analysis with sequential cuts on the discriminating variables, as shown in Fig. 1.16.

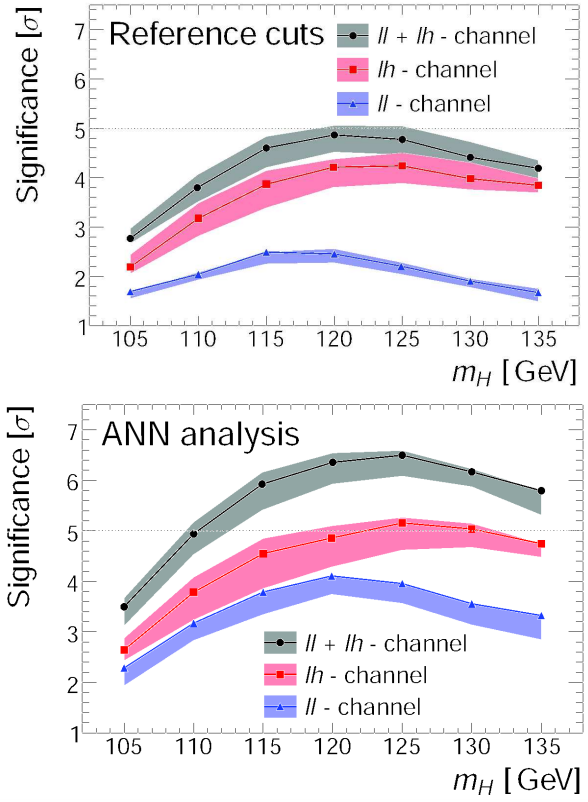

Figure 1.16: Discovery potential for the Higgs boson search in the $H \rightarrow \tau^+\tau^-$ decay channel, shown separately for the fully leptonic $\tau^+\tau^-$ decay mode ($\ell\ell$), semi-leptonic mode (ℓh) and their combination at an integrated luminosity of 30 fb^{-1} and a center-of-mass energy of 14 TeV. The results are obtained using the standard analysis with sequential cuts on the discriminating variables (top picture), as well as for neural network based analysis (bottom picture). The shaded bands indicate the effect of the experimental systematic uncertainties.

Higgs Bosons Beyond the Standard Model (MSSM)

The searches for the three neutral Higgs bosons predicted by the MSSM differ to some extent from the searches for the SM Higgs particle. The neutral Higgs decay modes into two intermediate gauge bosons are suppressed in MSSM, while the A and H boson decays into charged lepton pairs, $\mu^+\mu^-$ and $\tau^+\tau^-$ are enhanced compared to the Standard Model. The later decay channel has an about three hundred times higher branching ratio compared to the first one but is more difficult to reconstruct and provides a less precise Higgs mass determination.

Our studies of MSSM Higgs decays into two τ leptons are summarized in [28]. The dominant background contribution originates from the $Z \rightarrow \tau^+\tau^-$ and $t\bar{t}$ processes and can be suppressed by the requirements on the *b* quark jet reconstruction and large angular separation between the two decaying leptons. This channel provides the highest sensitivity reach for the neutral MSSM Higgs bosons.

Motivated by the excellent muon reconstruction in the ATLAS detector, we also study the prospects for the search in the channel with MSSM Higgs boson decays into two oppositely charged muons. The event selection criteria are optimized for the best discovery potential taknig into account the theoretical and experimental systematic uncertainties [29]. The invariant dimuon mass distribution after all analysis selection criteria is shown for the signal and dominant background processes in Fig. 1.17. The dominant $Z \rightarrow$

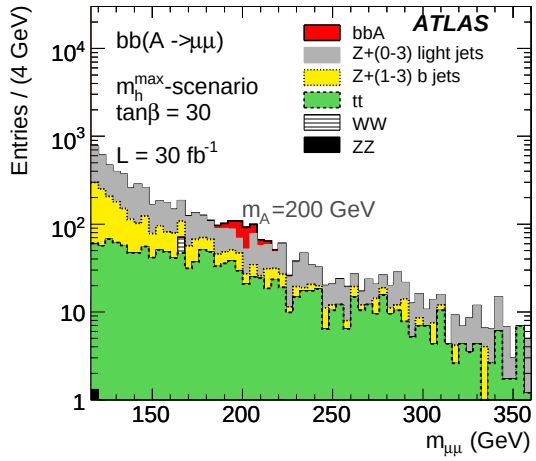

Figure 1.17: Invariant dimuon mass distributions of the main backgrounds and the *A* boson signal at masses M_A = 150, 200 and 300 GeV and tan β = 30, obtained for the integrated luminosity of 30 fb^{-1} at a center-of-mass energy of 14 TeV. Only events with at least one reconstructed *b* quark jet in the final state are selected.

$\mu^+\mu^-$ and $t\bar{t}$ background contributions are rather large compared to the signal and are subject to sizeable experimental systematic uncertainties, particularly with regard to the jet energy scale. It is therefore important to measure this background contribution with data. This can be done by combining the information from the side-bands of the invariant dimuon mass distribution with the measurements on the e^+e^- control sample. The later is motivated by an almost vanishing Higgs boson decay probability into two electrons, while the background contributions are similar for the dimuon and the dielectron final states. The expected ratio of invariant dielectron and dimuon mass distributions is shown in Fig. 1.18 after all analysis selection criteria and after correcting for the different electron and muon reconstruction and identification efficiency.

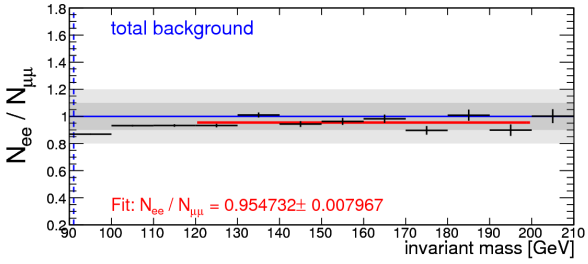

Figure 1.18: Ratio of the dilepton invariant mass distributions for the e^+e^- control sample and the total $\mu^+\mu^-$ background for the Higgs search in the $h/A/H \rightarrow \mu^+\mu^-$ channel, shown for an integrated luminosity of 4 fb^{-1} .

We perform a detailed study of the background estimation from data in [30, 31]. The presented method allows for a significant decrease of systematic uncertainties and thus in the imroved sensitivity reach for the MSSM Higgs boson search in the $\mu^+\mu^-$ decay channel. Especially during the initial phase of LHC running with the limited amount of data, the introduced control data samples are essential for obtaining reliable exclusion limits. The exclusion reach with early data at a center-of-mass collision energy of 7 TeV (See Fig. 1.19) has been evaluated in [32].

1.1.4 Searches for Supersymmetric Particles

Supersymmetry (SUSY) is the theoretically favoured model for physics beyond the Standard Model. The new symmetry uniting fermions and bosons predicts for each Standard Model particle a new supersymmetric partner with spin quantum number differing by 1/2. Supersymmetry provides a natural explanation for Higgs boson masses near the electroweak scale. In addition, the lightest stable supersimmetric particle is a good candidate for dark matter. If the mass scale of the SUSY is accessible at LHC, the squarks and gluinos (the superpartners of quarks and gluons with spin 0 and 1/2, respectively) will be copiously produced in *pp* collisions. In order to suppress the processes violating the barionic and leptonic quantum numbers, R-parity is introduced. The consequences of R-parity are that supersymmetric parti-

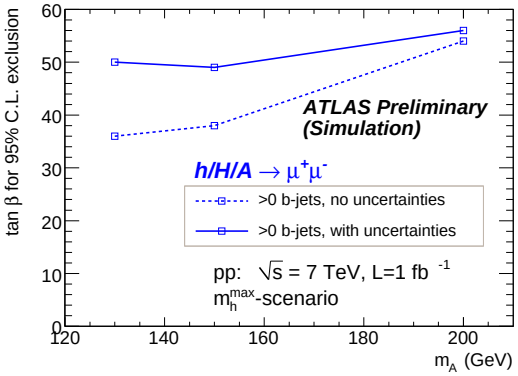

Figure 1.19: The $\tan\beta$ values needed for an exclusion of the neutral MSSM Higgs bosons shown as a function of the Higgs boson mass m_A for the analysis mode with at least one b-jet in the final state. An integrated luminosity of 1 fb^{-1} and a center-of-mass energy of 7 TeV are assumed. Dashed lines represent the results assuming zero uncertainty on the signal and background, while the full lines correspond to the results with both signal and background uncertainty taken into account.

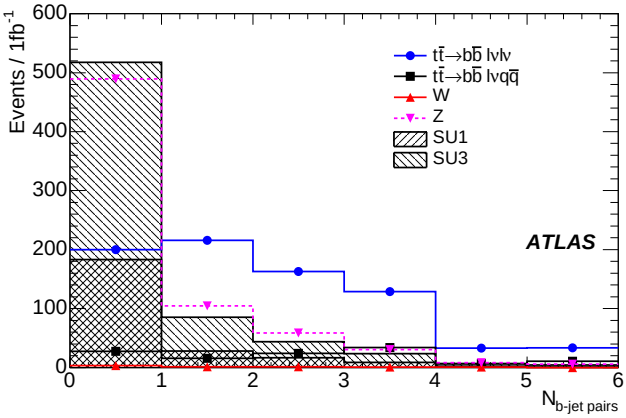

Figure 1.20: Number of b-jet pairs $N_{b-jetpairs}$ passing the kinematic requirements of $t\bar{t}$ process with both t-quarks decayed to b-quark, neutrino and lepton (electron or muon). The $N_{b-jetpairs} > 0$ region is mainly populated by $t\bar{t}$. This region is used as a "control sample" for the estimations of $t\bar{t}$ background with τ-lepton and non-identified electrons and muons in SUSY searches with one lepton. The bin $N_{b-jetpairs} = 0$ is filled by the gauge boson production processes and by the SUSY events simulated by two typical models labeled SU1 and SU3.

cles must be produced in pairs and each will decay to weakly interacting lightest supersymmetric particle via decay chains involving production of quarks and leptons. Therefore, the SUSY events are characterised by large transverse missing energy, high energetic hadron jets and leptons. The Standard Model processes with similar signature are top quarks ($t\bar{t}$) and gauge bosons (W and Z) production. In these processes the large transverse missing energy is originated from neutrino. These processes constitute the background to SUSY searches at LHC. Jet production from QCD process with "fake" transverse missing energy originated from jet energy mis-measurement is another important source of the background. Our studies are concentrated on the data-driven estimation of the backgrounds to SUSY searches, which is a key point of early discovery of SUSY by ATLAS detector.

With Monte Carlo simulations we have studied methods for determining the $t\bar{t}$ background from data [33]. The background estimation is performed by selection of SUSY-free "control sample" from which the prediction of background is derived. The $t\bar{t}$ production with top quark decays involving the τ leptons and non-reconstructed electrons or muons is estimated from similar events with identified muons and electron. The "control sample" composed mainly by events where both top quarks decayed to b-quark, neutrino and lepton (electron or muon) is selected by applying the set of kinematic constrains particular to this process. The resulting variable, denoting the number of b-jet pairs passing the kinematic constrains is used to separate the signal region into SUSY-dominated region and $t\bar{t}$-dominated region.

Similar strategy is used for isolation of the control sample with $t\bar{t}$ events with one top quark decayed to jet, neutrino and lepton (electron or muon), and the other top quark decayed to b-quark and two light quarks [34]. In this case the discriminating variable is the invariant mass of three close hadron jets, which is close to mass of the top quark for $t\bar{t}$ events.

The $t\bar{t}$ events with tau leptons produced be top-quark decay are reproduced by the events of the "control sample" by replacing the electron or muon with a tau lepton and simulating the tau lepton decay. Similar, the contribution with non-identified electron or muon is reproduced by treating the lepton as if it had not been identified.

References

[1] The MPI ATLAS group, *ATLAS Analysis*, Report to the Fachbeirat 1997–2003, (2004), 82-84.

[2] The MPI ATLAS group, *ATLAS Analysis*, Report to the Fachbeirat 2004–2006 Part II, (2006), 106-112.

[3] The MPP ATLAS group, *ATLAS Physics Analysis*, Annual Report 2006-2007 Part II, (2008), 107-116.

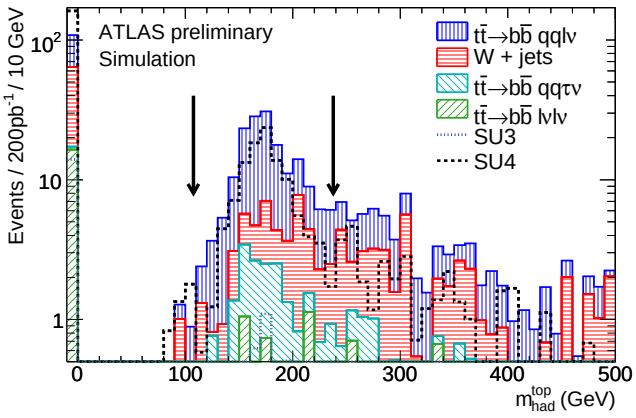

Figure 1.21: Distribution of invariant mass of tree close jets. This variable used for the selection of the "control sample" of $t\bar{t}$ events with one top quark decayed to jet, neutrino and lepton (electron or muon), and the other top quark decayed to b-quark and two light quarks. This "control sample" is used to derive the data-driven production of $t\bar{t}$ background in SUSY searches with no-lepton signatures. The arrows show the chosen window for this variable. The Standard Model contributions are shown by the stacked hatched histograms. The SUSY contribution for two typical SUSY models labeled as SU3 and SU4 are overlaid.

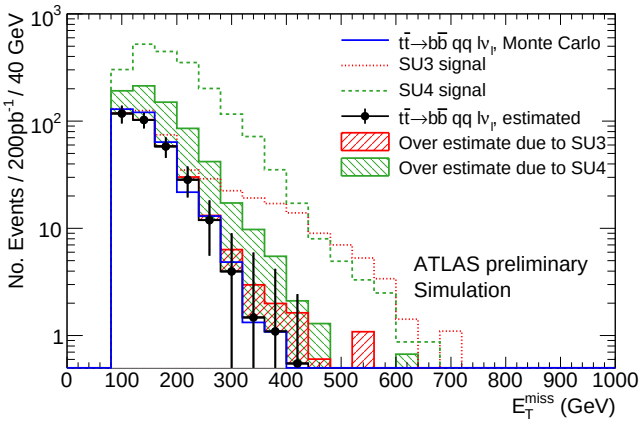

Figure 1.22: Distribution of transverse missing energy in $t\bar{t}$ events. The solid line shows the Monte Carlo estimate, circles show the result of data-driven estimation. The shaded histograms show the increase of data-driven estimates in the presence of SUSY signal (represented by SU3 and SU4 models) in the "control sample" and the dashed lines shows the SUSY signals stacked on the top of $t\bar{t}$ background.

[4] The ATLAS Collaboration, *Preliminary studies for the measurement of the inclusive muon spectrum in pp collisions at $\sqrt{s} = 7$ TeV with the ATLAS detector*, contribution to PLHC 2010, ATL-COM-CONF-2010-035.

[5] The ATLAS Collaboration, *Extraction of the prompt muon component in inclusive muons produced at $\sqrt{s} = 7$ TeV*, contribution to ICHEP 2010, ATL-COM-PHYS-2010-431.

[6] The ATLAS Collaboration, *Observation of prompt inclusive electrons in the ATLAS experiment at $\sqrt{s} = 7$ TeV*, contribution to ICHEP 2010, ATL-COM-PHYS-2010-422.

[7] The ATLAS Collaboration, *W/Z Cross-Sections*, contribution to ICHEP 2010, ATL-COM-PHYS-2010-475.

[8] G. Cortiana, T. Göttfert, P. Haefner, R. Nisius, P. Weigell, *Template Method for an early Top-Quark Mass Measurement in the $t\bar{t} \to$ lepton+jets Channel with ATLAS Data*, ATLAS internal note, ATL-PHYS-INT-2010-007, December 2009.

[9] The ATLAS Collaboration, G. Aad et al., *Expected Performance of the ATLAS Experiment Detector, Trigger and Physics*, CERN-OPEN-2008-020, pp898 (2008).

[10] P. Weigell, *Constrained Kinematic Fitting for a Top Quark Mass Determination in the Electron + Jets Channel at ATLAS*, Diploma thesis, Technische Universität München, MPP-2009-177, Oct 2009.

[11] E. Rauter, *Top Quark Mass Measurement: Prospects of Commissioning Studies for Early LHC Data in the ATLAS Detector*, Ph.D. thesis, Technische Universität München, MPP-2009-132, Jun 2009.

[12] The ATLAS Collaboration, *Prospects for the Measurement of the Top-Quark Mass using the Template Method with early ATLAS Data*, ATLAS public note, ATL-PHYS-PUB-2010-004, May 2010.

[13] G. Cortiana, R. Nisius, *Measurement of the Top-Quark Mass using the stabilized Mass Variable via the Template Method in the $t\bar{t} \to$ lepton+jets at ATLAS*, ATLAS internal note, ATL-PHYS-INT-2010-027, March 2010.

[14] S. Pataraia, *Studies on top quark-pair production in pp collisions at the Large Hadron Collider with the ATLAS experiment*, Ph.D. thesis, Technische Universität München, MPP-2009-181, Oct 2009.

[15] J. Schieck, *Early Top Physics with ATLAS*, ICPP Conference, Istanbul, Turkey, 27 - 31 Oct 2008, Balkan Phys. Lett. 17 (2009).

[16] G. Cortiana, *Prospects for the measurement of the top-quark mass with early ATLAS data*, TOP 2010 Conference, Brügge, Belgium, May 31 - Jun 4 2010, to be published in Nuovo Cim. C., MPP-2010-74

[17] The ATLAS Collaboration, *Higgs Boson, in Expected performance of the ATLAS experiment*, pages 1198-1511, CERN-OPEN-2008-020, CERN, Geneva, 2009, arXiv:hep-ex/0901.0512, MPP-2009-1.

[18] The ATLAS Collaboration, *ATLAS Sensitivity Prospects for Higgs Boson Production at the LHC Running at 7 TeV*, ATLAS public note (under approval), ATL-COM-PHYS-2010-373, CERN, Geneva, 2010.

[19] The ATLAS Collaboration, *Search for the Standard Model $H \to ZZ^{(*)} \to 4\ell$, in Expected performance of the ATLAS experiment*, pages 1243-1270, CERN-OPEN-2008-020, CERN, Geneva, 2009, arXiv:hep-ex/0901.0512, MPP-2009-1.

[20] Ch. Anastopoulos et al., *ATLAS sensitivity prospects for the Standard Model Higgs boson in the decay channel $H \to ZZ^{(*)} \to 4\ell$ at $\sqrt{s}$=10 and 7TeV* , ATLAS internal note, ATL-PHYS-INT-2010-062, CERN, Geneva, 2010.

[21] The ATLAS Collaboration, *Higgs Boson Searches in Gluon Fusion and Vector Boson Fusion using the $H \to WW$ Decay Mode, in Expected performance of the ATLAS experiment*, pages 1306-1332, CERN-OPEN-2008-020, CERN, Geneva, 2009, arXiv:hep-ex/0901.0512, MPP-2009-1.

[22] Steffen Kaiser, *Search for the Higgs Boson in the Process $pp \to Hqq, H \to WW$ with the ATLAS Detector*, Dissertation, Technische Universität München, 2010, MPP-2010-38.

[23] S. Kaiser, S. Horvat, O. Kortner, H. Kroha, *Impact of Pile-up on the Search for $H \to WW$ in VBF Production and Study of Track Jets for the Central Jet Veto*, ATLAS internal note (under approval), ATL-COM-PHYS-2010-197, CERN, Geneva, 2010.

[24] S. Kotov, S. Horvat, O. Kortner, H. Kroha, S. Mohrdieck-Möck; J. Yuan, *Search for the SM Higgs boson in the $H \to b\bar{b}$ decay channel in associated production with $t\bar{t}$ using neural network techniques*, ATLAS internal note, ATL-PHYS-INT-2008-027, CERN, Geneva, 2010.

[25] S. Horvat, O. Kortner, H. Kroha, S. Kotov, J. Yuan, *Feasibility study of the observability of the $H \to b\bar{b}$ in Vector Boson Fusion production with the ATLAS detector*, ATLAS internal note, ATL-PHYS-INT-2008-048, CERN, Geneva, 2010.

[26] The ATLAS Collaboration, *Search for the Standard Model Higgs Boson via Vector Boson Fusion Production Process in the Di-Tau Channels, in Expected performance of the ATLAS experiment*, pages 1271-1305, CERN-OPEN-2008-020, CERN, Geneva, 2009, arXiv:hep-ex/0901.0512, MPP-2009-1.

[27] Manfred Groh, *Study of the Higgs Boson Discovery Potential in the Process $pp \to Hqq, H \to \tau^+\tau^-$ with the ATLAS Detector*, Dissertation, Technische Universität München, 2009, MPP-2009-56.

[28] Georgios Dedes, *Study of the Higgs Boson Discovery Potential in the Process $pp \to H/A \to \mu^+\mu^-/\tau^+\tau^-$ with the ATLAS detector*, Dissertation, Technische Universität München, 2008, MPP-2008-32.

[29] The ATLAS Collaboration, *Search for the Neutral MSSM Higgs Bosons in the Decay Channel $A/H/h \to \mu^+\mu^-$, in Expected performance of the ATLAS experiment*, pages 1391-1418, CERN-OPEN-2008-020, CERN, Geneva, 2009, arXiv:hep-ex/0901.0512, MPP-2009-1.

[30] S. Stern, *Measurement of the $\mu^+\mu^-$ Background for Neutral MSSM Higgs Searches with the ATLAS Detector*, Diplomarbeit, Technische Universität München, 2010.

[31] S. Horvat, O. Kortner, H. Kroha, S. Stern, *Prospects for data-driven estimation of the $\mu^+\mu^-$ background for neutral MSSM Higgs searches in the decay channel $h/H/A \to \mu^+\mu^-$*, ATLAS internal note, ATL-PHYS-INT-2010-058, CERN, Geneva, 2010.

[32] S. Horvat, O. Kortner, H. Kroha, S. Stern, *ATLAS sensitivity prospects for the neutral MSSM Higgs bosons in the $H/A \to \mu^+\mu^-$ decay channel at $\sqrt{s}$ = 7 TeV*, ATLAS internal note, ATL-PHYS-INT-2010-057, CERN, Geneva, 2010.

[33] ATLAS collaboration, *Data-driven determinations of W, Z and top background to supersymmetry searches at the LHC*, in *Expected Performance of the ATLAS Experiment - Detector, Trigger and Physics*, p. 1525, 2009

[34] ATLAS collaboration, *Data-Driven Determination of $t\bar{t}$ Background to Supersymmetry Searches in ATLAS*, ATL-PHYS-PUB-2009-083, 2009